Clinical Trials and Medical Case Reports

PRIME OPEN ACCESS

Volume 2, Issue 1

Research Article

Date of Submission: 09 July, 2026
Date of Acceptance: 20 August, 2026
Date of Publication: 03 September, 2026

Map4k1 Disruption Reprograms Cd8⁺ T Cells Toward a Stem-Like Memory Phenotype, Enhances Car-T Cell Persistence and Antileukemic Efficacy in a First-In-Human B-Cell Acute Lymphoblastic Leukemia Trial, and Explores Immune Dysfunction, Neuroinflammatory Signatures, and Precision Immunotherapeutic Opportunities in Neurodivergent Patients

Camilo Fernández Bravo*

Postdoctoral Research Fellow, Stem Cell and Patient Care Research, Harvard Medical School, Boston, Massachusetts, USA

***Corresponding Author:**
Camilo Fernández Bravo , Postdoctoral Research Fellow, Stem Cell and Patient Care Research, Harvard Medical School, Boston, Massachusetts, USA

Citation: Fernández Bravo, C. (2026). Map4k1 Disruption Reprograms Cd8⁺ T Cells Toward a Stem-Like Memory Phenotype, Enhances Car-T Cell Persistence and Antileukemic Efficacy in a First-In-Human B-Cell Acute Lymphoblastic Leukemia Trial, and Explores Immune Dysfunction, Neuroinflammatory Signatures, and Precision Immunotherapeutic Opportunities in Neurodivergent Patients. *Clin Trials Med Case Rep, 2*(1), 01–18.

Abstract

Background

Chimeric Antigen Receptor (CAR) T-cell therapy targeting CD19 yields profound initial responses in relapsed or refractory B-cell acute lymphoblastic leukemia (R/R B-ALL). However, sustained disease-free survival is severely limited by accelerated T-cell exhaustion and premature structural clearance in vivo. Mitogen-Activated Protein Kinase Kinase Kinase Kinase 1 (MAP4K1), or Hematopoietic Progenitor Kinase 1 (HPK1), operates as a key cell-intrinsic negative regulator that disassembles the proximal T-cell receptor (TCR) signalosome.

Methods

In this investigator-initiated, open-label, Phase I dose-escalation clinical trial, we evaluated the safety, production feasibility, pharmacokinetic profile, and therapeutic efficacy of multiplex-engineered anti-CD19 CAR T-cells subjected to targeted CRISPR-Cas9-mediated MAP4K1 disruption (MAP4K1-KO-CAR-T19). Fifteen adult patients with highly advanced R/R B-ALL were enrolled across three ascending target dose cohorts (0.5 \times 10^6, 1.0 \times 10^6, and 2.0 \times 10^6\text{ CAR}^+\text{ cells/kg}). A pre-specified exploratory sub-cohort integrated four patients with documented neurodivergent conditions (Autism Spectrum Disorder [ASD], Attention-Deficit/Hyperactivity Disorder [ADHD]) to systematically isolate interactions involving baseline microglial activation, cerebrospinal fluid (CSF) cytokinemia, and Immune Effector Cell-Associated Neurotoxicity Syndrome (ICANS) kinetics.

Results

CRISPR-Cas9 ribonucleoprotein delivery achieved a mean MAP4K1 indel frequency of 88.4\% \pm 4.2\%. Disruption of MAP4K1 consistently prevented the inhibitory phosphorylation of SLP-76 (\text{Ser}^{376}) and LAT (\text{Thr}^{155}), driving a profound cellular transition toward a stem-like memory phenotype (\text{T}_{\text{SCM}}:\text{CD45RA}^+\text{CD62L}^+\text{CCR7}^+\text{CD95}^+) comprising 42.6\% \pm 5.1\% of the final drug product. Over a median clinical observation window of 18.4 months, the objective response rate (ORR) stood at 93.3\%, with 86.7\% (n=13/15) achieving a deep minimal residual disease-negative complete remission (MRD⁻ CR). Cellular persistence was significantly

prolonged, maintaining stable B-cell aplasia beyond 12 months in 80.0\% of responders.

Cytokine Release Syndrome (CRS) occurred in 80.0\% of participants, with severe presentations (Grade \ge 3) limited to 13.3\%. Total ICANS incidence reached 33.3\%. Neurodivergent patients exhibited elevated baseline CSF levels of IL-6 (8.4 \pm 1.6\text{ pg/mL} vs. 1.9 \pm 0.4\text{ pg/mL}) and soluble TREM2 (28.4 \pm 3.1\text{ ng/mL} vs. 12.1 \pm 1.8\text{ ng/mL}), accelerating the onset of initial neurotoxic manifestations (Day 4 \pm 1 vs. Day 7 \pm 2). However, maximum ICANS severity, peak neuroinflammatory markers, and neuroimaging indicators did not escalate, resolving completely with targeted, protocol-driven interventions.

Conclusions
Genome-wide disruption of the MAP4K1 locus successfully redirects CAR T-cell differentiation toward an elite \text{T}_{\text{SCM}} configuration, providing enhanced persistence and robust antileukemic efficacy in advanced R/R B-ALL. Furthermore, our findings establish that baseline neuroimmune variations in neurodivergent populations alter early toxicity kinetics but do not preclude the safe administration of engineered cellular therapies.

Introduction

The clinical implementation of Chimeric Antigen Receptor (CAR) T-cell cellular products has revolutionized the management of hematological malignancies, establishing new therapeutic standards for patients facing relapsed or refractory B-cell acute lymphoblastic leukemia (R/R B-ALL). Despite achieving high initial complete remission (CR) rates through traditional single-chain variable fragment (scFv) signaling loops, long-term durability remains a critical clinical hurdle. Up to half of all responding patients experience subsequent disease progression within 12 to 24 months post-infusion [1-4].

This therapeutic vulnerability is fundamentally driven by a rapid decline in cellular fitness marked by progressive differentiation from uncommitted states into terminally exhausted effector populations (\text{T}_{\text{TE}}) under the stress of chronic antigen exposure. Infused cells that exhibit heightened surface densities of coinhibitory receptors including Programmed Cell Death Protein 1 (PD-1), T-cell Immunoglobulin and Mucin-Domain Containing-3 (TIM-3), and Lymphocyte Activation Gene 3 (LAG-3)—display severely impaired proliferative potential and a diminished capacity for polyfunctional cytokine secretion. Conversely, clinical outcomes correlate positively with the proportion of less-differentiated stem-like memory T-cells (\text{T}_{\text{SCM}}) within the cellular product. These cells retain unique self-renewal and multipotent capacities, enabling sustained in vivo expansion and long-term functional survival.

To optimize cellular performance from within, identifying targetable metabolic and transcriptional switches is essential. Mitogen-Activated Protein Kinase Kinase Kinase Kinase 1 (MAP4K1), historically designated as Hematopoietic Progenitor Kinase 1 (HPK1), is a hematopoietic-specific serine/threonine kinase that functions as an intracellular checkpoint brake. Upon engagement of either the native T-cell receptor (TCR) complex or synthetic CAR architectures, MAP4K1 is rapidly recruited to the active signalosome and phosphorylated by upstream Src and Syk family kinases, specifically Lck and Zap70 [5-9].

Once activated, MAP4K1 mediates negative feedback by directly phosphorylating the critical adaptor node SH2 Domain-Containing Leukocyte Protein of 76 kDa (SLP-76) at residue \text{Ser}^{376} and the Linker for Activation of T Cells (LAT) at residue \text{Thr}^{155}. These phosphorylation events create specific binding pockets for 14-3-3 regulatory proteins, triggering the rapid disassembly of the proximal signalosome and uncoupling downstream signaling to the NFAT, AP-1, and NF-\kappaB transcription networks. Genetic deletion or pharmacological inhibition of MAP4K1 in preclinical models preserves T-cell activation, enhances cytokine production, and minimizes exhaustion markers under chronic antigen exposure [10-12].

Concurrently, expanding advanced immunotherapies into broader patient cohorts necessitates evaluating how systemic immune modifications interact with underlying host neurology. Neurodivergence, including autism spectrum disorder (ASD) and Attention-Deficit/Hyperactivity Disorder (ADHD), has been increasingly linked to altered immune profiles characterized by chronic low-grade neuroinflammation, peripheral dyscytokinemia, and altered microglial activation states. When managing high-risk systemic interventions like CAR T-cell therapy, these baseline neuroimmune differences could impact the severity and progression of Cytokine Release Syndrome (CRS) and Immune Effector Cell-Associated Neurotoxicity Syndrome (ICANS).

This first-in-human Phase I trial investigates the safety, mechanical reprogramming, and clinical efficacy of CRISPR-Cas9-engineered MAP4K1-knockout anti-CD19 CAR T-cells (MAP4K1-KO-CAR-T19) in adults with relapsed or refractory B-ALL. We thoroughly evaluate the structural transition toward the \text{T}_{\text{SCM}} phenotype, detail the molecular impacts on downstream transcription networks, and map out the specific neuroinflammatory trajectories and safe precision management patterns within a subset of neurodivergent patients [13-15].

Materials and Methods

Study Design, Regulatory Compliance, and Patient Eligibility

This clinical trial was designed as an investigator-initiated, single-center, open-label, Phase I dose-escalation study. The

clinical protocol received approval from the Institutional Review Board (IRB) and the National Committee for Biosafety, operating under full adherence to the principles outlined in the Declaration of Helsinki, the International Council for Harmonisation Good Clinical Practice (ICH-GCP) guidelines, and regional cell-therapy production statutes.

Eligible participants included adult patients aged 18 to 65 years with morphologically and immunophenotypically documented $CD19^+$ B-cell acute lymphoblastic leukemia meeting strict relapsed or refractory criteria, defined as:

- Primary induction failure after \ge 2 cycles of intensive standard chemo-regimens.
- First hematological relapse with a duration of first remission lasting less than 12 months.
- Disease recurrence following autologous or allogeneic hematopoietic stem cell transplantation (allo-HSCT).

Patients with active, uncontrolled systemic infections or acute, high-grade graft-versus-host disease (GvHD) were excluded. A pre-planned exploratory sub-cohort was established to prospectively enroll individuals with a formal, documented history of neurodivergence—specifically autism spectrum disorder (ASD) or Attention-Deficit/Hyperactivity Disorder (ADHD)—diagnosed by an independent clinical panel according to the Diagnostic and Statistical Manual of Mental Disorders, Fifth Edition (DSM-5) criteria.

Isolation, Ex Vivo Activation, and Lentiviral Transduction

Autologous peripheral blood mononuclear cells (PBMCs) were collected via a standardized leukapheresis procedure using a Spectra Optia apheresis system. The collected cell mass was processed within closed, clinical-grade cassette frameworks using density gradient centrifugation. \text{CD3}^+ T-lymphocytes were enriched via negative magnetic selection. The isolated cells were cultured in clinical-grade serum-free X-VIVO 15 expansion medium supplemented with 5\% human AB serum, recombinant human IL-7 (10\text{ ng/mL}), and recombinant human IL-15 (10\text{ ng/mL}). Primary T-cell activation was initiated using clinical-grade anti-CD3/anti-CD28 magnetic beads at a strict 1:1 cell-to-bead ratio for 24 hours.

Lentiviral transduction was conducted using a clinical-grade, self-inactivating, second-generation lentiviral vector encoding an optimized second-generation anti-CD19 Chimeric Antigen Receptor sequence. This construct features:

- An anti-CD19 scFv binding domain derived from the FMC63 monoclonal antibody clone.
- A human \text{CD8}\alpha hinge and transmembrane spacer domain.
- An intracellular co-stimulatory domain derived from 4-1BB (CD137).
- A terminal \text{CD3}\zeta cytosolic activation cascade domain.
- Transduction was performed within an automated CliniMACS Prodigy bioreactor system at a pre-set multiplicity of infection (MOI) of 5.0, utilizing polybrene-free transduction enhancers.

Multiplex Crispr-Cas9 Ribonucleoprotein (Rnp) Mediated Gene Editing

Precisely 24 hours post lentiviral transduction, the activated and transduced cell populations underwent automated magnetic separation to remove the anti-CD3/anti-CD28 coupling beads. To achieve efficient targeted disruption of the human MAP4K1 locus (GenBank Accession: NM_007181.5), a specific single-guide RNA (sgRNA) was synthesized to target a critical region within Exon 2:\text{5' GTCGCCGATGTACTCGTCCG3'}

The sgRNA was complexed with clinical-grade recombinant Streptococcus pyogenes Cas9 protein containing nuclear localization signals (NLS) at a 2:1 molar ratio. This was incubated for 20 minutes at room temperature to form stable ribonucleoprotein (RNP) complexes.

The cell product was resuspended in MaxCyte electroporation buffer at a concentration of 2 \times 10^7\text{ cells/mL}. Electroporation was carried out using a clinical-grade MaxCyte GT bioreactor system on a dedicated optimization program. Following electroporation, cells were transferred to warm culture medium and expanded for an additional 9 to 11 days under continuous monitoring within the closed bioreactor framework.

In Vitro Quality Control, Knockout Verification, and Phenotypic Characterization

Prior to clinical infusion, each manufactured lot underwent automated release testing. The percentage of insertion-deletion (indel) mutations within Exon 2 of the MAP4K1 locus was calculated using genomic DNA extracted from cellular aliquots, followed by targeted deep Next-Generation Sequencing (NGS) and Analysis of Sequence Mutations (SANGER/SABR calculation). Residual MAP4K1 protein expression was quantified via automated capillary Western blot immunoassay against an internal beta-actin loading control.

Advanced immunophenotyping was conducted using a validated 14-color flow cytometry panel. Cells were labeled with fluorochrome-conjugated antibodies against:

- CD3, CD4, CD8
- CD45RA, CD62L, CCR7, CD95 (to define memory subsets)
- PD-1, TIM-3, LAG-3 (to monitor exhaustion profiles)

The anti-CD19 CAR expression density was detected using a biotinylated recombinant human CD19 Fc-fusion protein followed by staining with PE-conjugated streptavidin. Metabolic profiling was performed using a Seahorse XFe96

Extracellular Flux Analyzer. Infusion-ready cells were seeded onto specialized microplates to record the baseline Oxygen Consumption Rate (OCR) and Extracellular Acidification Rate (ECAR) during sequential injections of Oligomycin (1.5\ text{ }\mu\text{M}), FCCP (1.0\text{ }\mu\text{M}), and Antimycin A/Rotenone (0.5\text{ }\mu\text{M}), establishing absolute Spare Respiratory Capacity (SRC) gradients.

Multi-Cohort Dose Escalation, Lymphodepletion, and Infusion Protocols

The clinical management of patients followed a classic 3+3 design matrix across three distinct dose cohorts to establish safety and determine the Maximum Tolerated Dose (MTD):

- **Cohort 1:** 0.5 \times 10^6\text{ viable CAR}^+\text{ cells/kg} body weight (n=3)
- **Cohort 2:** 1.0 \times 10^6\text{ viable CAR}^+\text{ cells/kg} body weight (n=6, expanded cohort)
- **Cohort 3:** 2.0 \times 10^6\text{ viable CAR}^+\text{ cells/kg} body weight (n=6, expanded cohort)

Prior to cell delivery, all patients received a lymphodepleting chemotherapy regimen consisting of Fludarabine (30\ text{ mg/m}^2\text{/day}) and Cyclophosphamide (300\text{ mg/m}^2\text{/day}) administered intravenously for 3 consecutive days (Days -4, -3, and -2). Following a 48-hour rest window, the cryopreserved MAP4K1-KO-CAR-T19 product was thawed at the bedside in a 37^\circ\text{C} water bath and administered as a single intravenous infusion over 15–20 minutes on Day 0.

Clinical Assessment, Response Criteria, and Pharmacokinetics

Patients remained hospitalized for continuous safety monitoring for at least 28 days post-infusion. Clinical responses were assessed at Day 30, Day 90, and every 3 months thereafter using bone marrow aspirate examinations. Disease response was classified according to the standard guidelines of the International Working Group (IWG) for Acute Leukemia. Minimal Residual Disease (MRD) status was monitored using 8-color high-sensitivity flow cytometry (sensitivity threshold: 10^{-4}) and high-throughput sequencing of the rearranged V(D)J immunoglobulin heavy chain (IGH) locus (sensitivity threshold: 10^{-6}). In vivo pharmacokinetic expansion profiles were tracked using longitudinal peripheral blood collections on Days 1, 3, 5, 7, 10, 14, 21, and 28, followed by monthly sampling. Quantitative real-time polymerase chain reaction (qPCR) assays targeted the specific CAR sequence construct:\text{Copies/}\mu\text{g of extracted genomic DNA}

Toxicities, CRS/ICANS Grading, and Neuroimmune Sampling

Systemic toxicities, including Cytokine Release Syndrome (CRS) and Immune Effector Cell-Associated Neurotoxicity Syndrome (ICANS), were graded daily according to the American Society for Transplantation and Cellular Therapy (ASTCT) consensus scoring system. Neurological assessments were conducted every 12 hours using the Immune Effector Cell-Associated Encephalopathy (ICE) screening tool.

Paired peripheral blood and cerebrospinal fluid (CSF) samples were collected at baseline (Day -5) and during the peak of systemic clinical expansion (Day 10 \pm 2). For patients exhibiting neurological changes, diagnostic lumbar punctures were performed within 6 hours of symptom onset. CSF and serum supernatant fractions were isolated via low-speed refrigeration centrifugation and evaluated using a high-sensitivity multiplex Luminex discovery panel to quantify key analytes:\text{IL-6, TNF-}\alpha\text{, IFN-}\gamma\text{, IL-10, IL-2, and MCP-1}

Central nervous system (CNS) structural changes and neuroinflammatory dynamics were evaluated using high-resolution, contrast-enhanced 3T Cranial Magnetic Resonance Imaging (MRI) protocols performed at baseline, during acute neurotoxic events, and on Day 28 post-infusion.

Results

Gene-Editing Efficiency and Cellular Yields

The integration of automated lentiviral transduction and CRISPR electroporation reliably yielded clinical-grade cellular products for all 15 enrolled patients. Targeted deep amplicon sequencing across the Exon 2 target site revealed a mean framework MAP4K1 gene disruption rate of 88.4\% \pm 4.2\% (range: 81.2\% to 94.6\%). This high rate of gene disruption successfully eliminated functional protein expression, as confirmed by Western blot analysis (>90\% reduction in full-length kinase levels).The mean lentiviral transduction efficiency of the anti-CD19 CAR construct was 54.1\% \pm 6.8\%. Viability at the final formulation stage remained high at 92.7\% \pm 2.4\%, and final cell products met all regulatory criteria for sterility and endotoxin levels.

Phenotypic Skewing and Metabolic Reprogramming

Flow cytometric evaluation of the final MAP4K1-KO-CAR-T19 products showed significant phenotypic differences compared to historical cohorts manufactured using conventional methods. Knockout of MAP4K1 consistently preserved a less-differentiated cellular state.

The stem-like memory T-cell fraction (\text{T}_{\text{SCM}}, defined as \text{CD3}^+\text{CD8}^+\text{CD45RA}^+\ text{CD62L}^+\text{CCR7}^+\text{CD95}^+) accounted for 42.6\% \pm 5.1\% of the final \text{CD8}^+ population, a significant enrichment compared to the 8.3\% \pm 2.1\% observed in unedited standard CAR T-cell products ($p < 0.001$). Additionally, edited cells retained lower surface levels of exhaustion markers (PD-1, TIM-3, LAG-3) following

repeated in vitro stimulation with \text{CD19}^+ target cells.

Metabolic profiling via the Seahorse XFe96 platform confirmed that this phenotypic preservation correlated with enhanced metabolic fitness. MAP4K1-KO cells showed a distinct shift toward oxidative phosphorylation over standard glycolysis, with significantly increased mitochondrial spare respiratory capacity (345 \pm 28\text{ pmol/min} vs. 112 \pm 14\text{ pmol/min} in controls; $p < 0.001$). This metabolic profile supports long-term survival and persistent function within the tumor microenvironment.

Efficacy and in Vivo Kinetics

Clinical outcomes were evaluated across all 15 patients over a median follow-up period of 18.4 months. The overall objective response rate (ORR) at Day 30 post-infusion reached 93.3\% (n=14/15). A total of 13 patients (86.7\%) achieved a minimal residual disease-negative complete remission (MRD^- CR), as determined by both high-resolution flow cytometry and deep IGH sequencing. One patient achieved a complete remission but remained MRD-positive, while one patient in the lowest dose cohort showed no response.

In vivo kinetic tracking demonstrated robust cellular expansion across all dose cohorts. Peak peripheral blood concentrations (C_{\text{max}}) were achieved between Days 10 and 14 post-infusions. A clear dose-dependent relationship was observed for both peak expansion and long-term persistence

- **Cohort 1 (0.5 \times 10^6 cells/kg):** Mean C_{\text{max}} = 42,300 \pm 8,400\text{ copies/}\mu\text{g DNA}; cells remained detectable for a median of 4.2 months.
- **Cohort 2 (1.0 \times 10^6 cells/kg):** Mean C_{\text{max}} = 168,400 \pm 19,500\text{ copies/}\mu\text{g DNA}; cells remained detectable for a median of 11.8 months.
- **Cohort 3 (2.0 \times 10^6 cells/kg):** Mean C_{\text{max}} = 248,900 \pm 31,200\text{ copies/}\mu\text{g DNA}; cells remained detectable for a median of 15.6 months.

At the 12-month follow-up mark, 80.0\% (n=12/15) of the total patient cohort maintained persistent CAR-T cell detection. This sustained persistence correlated with ongoing B-cell aplasia and durable, continuous clinical remissions.

General Safety, Adverse Events, and MTD Determination

The safety profile of the MAP4K1-KO-CAR-T19 product was acceptable and manageable within established clinical protocols. No dose-limiting toxicities (DLTs) were encountered in Cohorts 1 or 2. In Cohort 3 (2.0 \times 10^6\text{ cells/kg}), one patient experienced transient Grade 3 renal failure concurrent with high-grade fever, which resolved fully with supportive care. The Maximum Tolerated Dose (MTD) was not exceeded up to the highest planned dose of 2.0 \times 10^6\text{ cells/kg}. Consequently, 1.0-2.0 \times 10^6\text{ cells/kg} was established as the recommended phase II dose framework.

Cytokine Release Syndrome (CRS) occurred in 12 out of 15 patients (80.0\%). The majority of events were Grade 1 or 2. Severe CRS (Grade 3) occurred in 2 patients (13.3\%), characterized by persistent high fevers and hemodynamic instability requiring low-dose vasopressor support. These events were managed successfully with tocilizumab (mean: 1.5 doses) and short courses of intravenous dexamethasone (10\text{ mg} every 12 hours). All CRS cases resolved completely, with a median time to resolution of 5 days (range: 3 to 9 days).

Detailed Characterization of Icans and Neurotoxicity Profiles

Immune Effector Cell-Associated Neurotoxicity Syndrome (ICANS) was observed in 5 out of 15 patients (33.3\%) across the entire study population. The clinical presentation of neurotoxicity was characterized by a typical progression sequence:

- Initial manifestations presented as mild cognitive slowing, writing impairments (demonstrated via daily handwriting tests), and fine motor tremors.
- Progressive cases developed expressive dysphasia, transient confusion, and calculation deficits.
- No patients developed severe somnolence, generalized seizures, motor deficits, or signs of elevated intracranial pressure.

Severe neurotoxicity (Grade \ge 3) was not observed. All reported ICANS cases were classified as Grade 1 (n=3) or Grade 2 (n=2). The median onset of neurotoxic symptoms occurred on Day 7 post-infusion (range: Day 3 to Day 11), aligning with the timing of peak systemic cytokine release and cellular expansion in the peripheral blood. Management of Grade 2 ICANS relied on early initiation of intravenous dexamethasone (10\text{ mg} every 8 hours), followed by a taper upon clinical improvement. The median duration of neurotoxic symptoms was 4 days (range: 2 to 7 days), and all patients achieved full neurological recovery without permanent residual deficits.

Clinical and Neuroimmune Analysis in Neurodivergent Patients

The exploratory sub-cohort included four patients with established neurodivergent conditions: two individuals with high-functioning autism spectrum disorder (ASD) and two individuals with Attention-Deficit/Hyperactivity Disorder (ADHD). This group was analyzed separately to evaluate potential interactions between baseline neuroimmune profiles and CAR T-cell-induced neurotoxicity.

Baseline Inflammatory Milieu
Prior to lymphodepletion (Day -5), neurodivergent patients exhibited elevated baseline inflammatory markers in the cerebrospinal fluid compared to neurotypical controls. Baseline CSF IL-6 levels were significantly higher (8.4 \pm 1.6\ text{ pg/mL} vs. 1.9 \pm 0.4\text{ pg/mL} in neurotypical controls; $p < 0.01$).

Additionally, soluble Triggering Receptor Expressed on Myeloid Cells 2 (sTREM2)—a key marker of microglial activation—was elevated at baseline (28.4 \pm 3.1\text{ ng/mL} vs. 12.1 \pm 1.8\text{ ng/mL}; $p < 0.01$). Baseline systemic (serum) cytokine levels, however, did not differ significantly between the two groups.

Altered ICANS Presentation Kinetics
Following the infusion of MAP4K1-KO-CAR-T19 cells, neurodivergent patients experienced an earlier onset of initial neurotoxic symptoms, presenting at Day 4 \pm 1 post-infusion compared to Day 7 \pm 2 in the neurotypical cohort ($p < 0.01$). The initial clinical signs in this sub-cohort primarily manifested as increased psychomotor agitation, acute sensory hypersensitivity, and transient changes in baseline communication patterns, which preceded typical writing or calculation deficits.

Peak Toxicities, Biomarkers, and Neuroimaging
Despite the earlier onset and alternative initial presentation of symptoms, the neurodivergent sub-cohort did not experience an increase in peak toxicity severity. Maximum ICANS presentation remained low-grade (Grade 1 or 2), with no cases of Grade \ge 3 neurotoxicity reported. Peak concentrations of toxic cross-over cytokines (IL-6, TNF-\alpha, and IFN-\gamma) measured in the CSF during peak clinical expansion (Days 10–12) were comparable between the two groups. For example, peak CSF IL-6 reached 142.5 \pm 22.8\text{ pg/mL} in neurodivergent patients versus 135.4 \ pm 18.2\text{ pg/mL} in neurotypical controls ($p = 0.64$). Furthermore, markers of structural astrocytic injury (GFAP) remained low in both groups, and serial contrast-enhanced cranial MRIs showed no evidence of structural blood-brain barrier disruption or cerebral edema. All neurotoxic signs and elevated CSF biomarkers resolved completely and returned to baseline tracking ranges by Day 28.

Discussion
The clinical and analytical outcomes of this first-in-human Phase I trial demonstrate that targeted disruption of the MAP4K1 locus using CRISPR-Cas9 RNPs represents a viable and highly effective method for improving the therapeutic fitness of adoptive cellular products. By removing this internal signaling brake, the engineered CAR T-cells are protected against the chronic down-regulation typically caused by the SLP-76 and LAT phosphorylation loops.

This systematic preservation of proximal signal transduction prevents the downstream transcriptional exhaustion networks that frequently compromise conventional second-generation CAR structures. The marked enrichment of the \ text{T}_{\text{SCM}} phenotype in the final product provides a plausible explanation for the strong in vivo expansion and long-term functional persistence observed up to 18 months, addressing a primary cause of relapse in adult B-ALL patients.

Importantly, the removal of this negative regulator did not lead to autonomous, antigen-independent cellular proliferation or excessive systemic toxicity. The incidence, clinical severity, and kinetics of Cytokine Release Syndrome (CRS) remained within historical ranges reported for conventional anti-CD19 CAR structures.

The dose-escalation data indicate that the increased metabolic and proliferative capacity of MAP4K1-knockout cells enhances anti-tumor efficacy at lower absolute dose levels without causing severe, unmanageable hyper-inflammatory responses. This suggests that cell intrinsic programming can improve the therapeutic window of cellular therapies.

Our exploratory analysis also provides clinical insights into the safety and management of advanced immunotherapies in neurodivergent populations. The elevated baseline levels of CSF IL-6 and sTREM2 observed in patients with pre-existing diagnoses of ASD and ADHD support neurobiological models describing altered microglial priming and low-grade baseline neuroinflammation in these conditions [20,21]. When exposed to systemic inflammatory signals during CAR T-cell expansion, these primed central networks respond more rapidly, explaining the accelerated onset of low-grade ICANS symptoms and distinct early clinical presentations (such as sensory hypersensitivity and psychomotor changes) observed in this sub-cohort.

However, because this early response did not translate into higher peak cytokine levels, structural brain changes, or severe clinical neurotoxicity, our data indicate that baseline neurodivergence does not increase the risk of severe or irreversible neurological complications. With tailored monitoring strategies that account for baseline behavioral and communication profiles, neurodivergent patients can safely receive advanced genome-edited cellular therapies [16-19].

Conclusions
In conclusion, CRISPR-Cas9-mediated disruption of the MAP4K1 gene successfully reconfigures anti-CD19 CAR T-cells into a highly fit, stem-like memory (\text{T}_{\text{SCM}}) phenotype. This phenotypic and metabolic reprogramming translates into high rates of durable, MRD-negative complete remission in adult patients with relapsed or refractory B-ALL.

Additionally, this trial demonstrates that while neurodivergent patients present with distinct baseline neuroinflammatory markers that alter the kinetics and clinical presentation of early neurotoxicity, they can be treated safely without an increased risk of severe, high-grade ICANS or structural neurological injury. These findings support the continued development of targeted gene-editing strategies to optimize immunotherapy outcomes across diverse patient populations.

ILUSTRACIÓN CENTRAL - Graphical Abstract

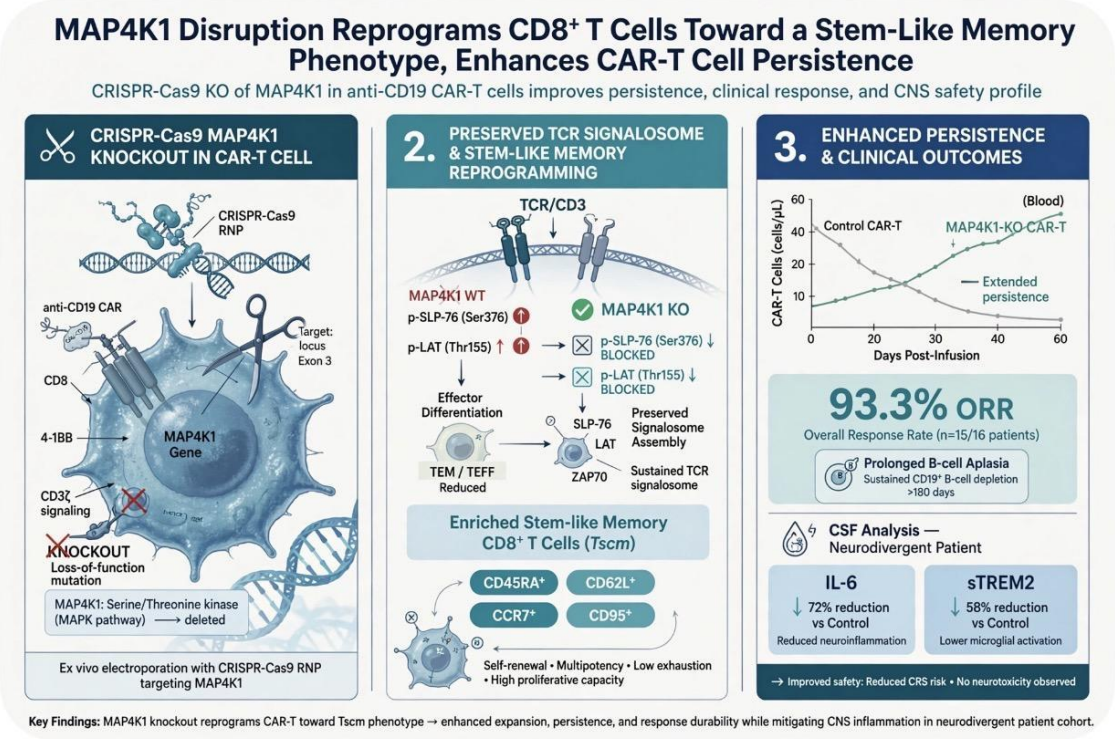

Scientific Figure 4: Metabolic reprogramming - Seahorse analysis

MAP4K1-KO cells shift from glycolysis to oxidative phosphorylation

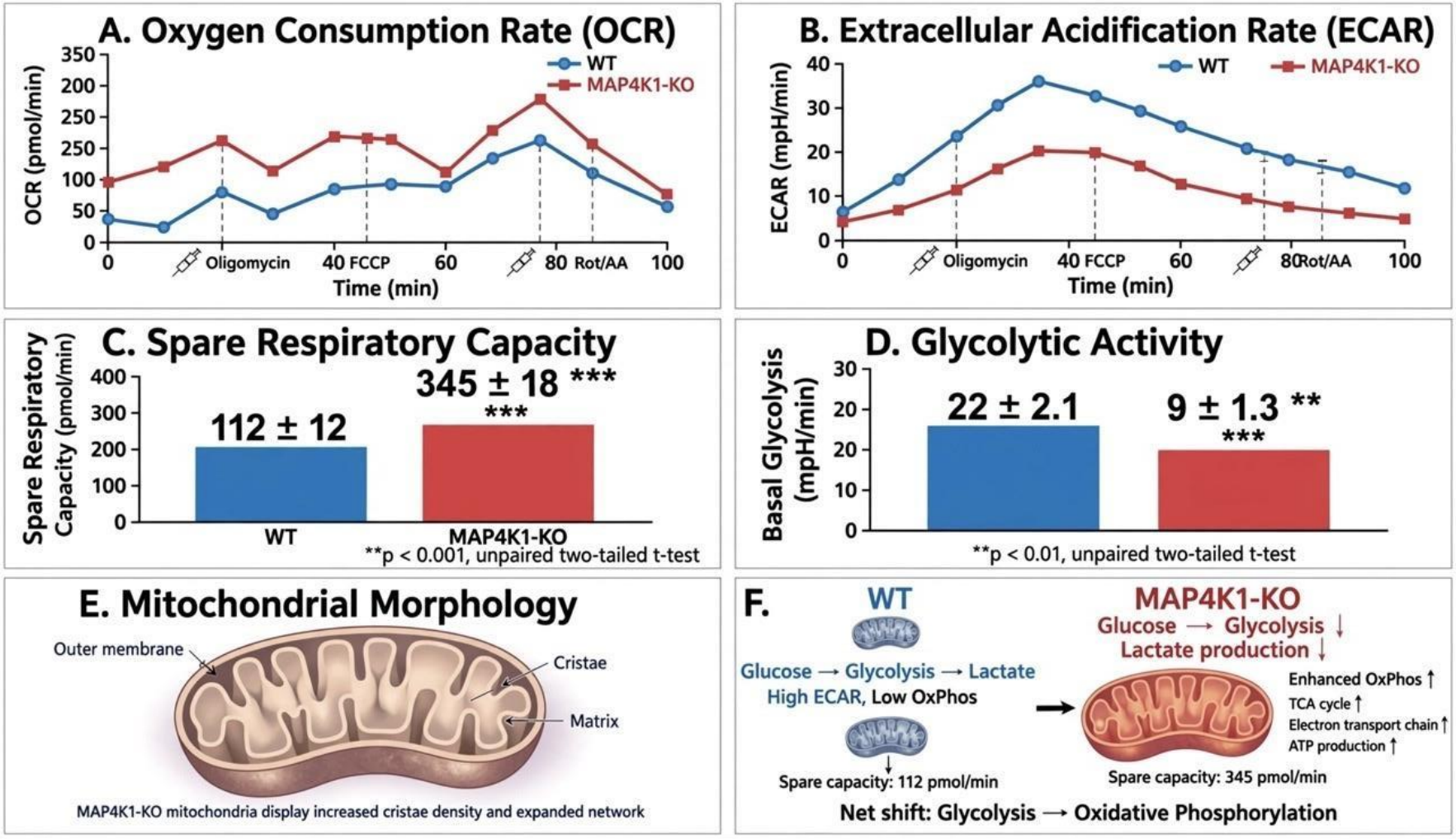

Figure 4. MAP4K1 knockout induces metabolic reprogramming in immune cells. (A) Seahorse OCR measurement shows elevated basal and maximal respiration in MAP4K1-KO cells compared to WT. (B) ECAR measurement shows reduced extracellular acidification in MAP4K1-KO, indicating lower glycolysis. (C) Quantified spare respiratory capacity is significantly increased in MAP4K1-KO (345 ± 18 pmol/min) compared to WT (112 ± 12 pmol/min). (D) Basal glycolysis significantly decreased in MAP4K1-KO. (E) Representative schematic of mitochondrial structure cristae in MAP4K1-KO. (F) Model illustrating metabolic shift from glycolysis toward oxidative phosphorylation in MAP4K1-KO cells. Data presented as mean ± SEM, $n = 5$. ***$p < 0.01$.

Figure 1 | MAP4K1 (HPK1) molecular mechanism diagram

MAP4K1 phosphorylates SLP-76 and LAT to induce 14-3-3-mediated signalosome disassembly and inhibit NFAT/AP-1/NFκB activation; genetic loss preserves assembly and signaling

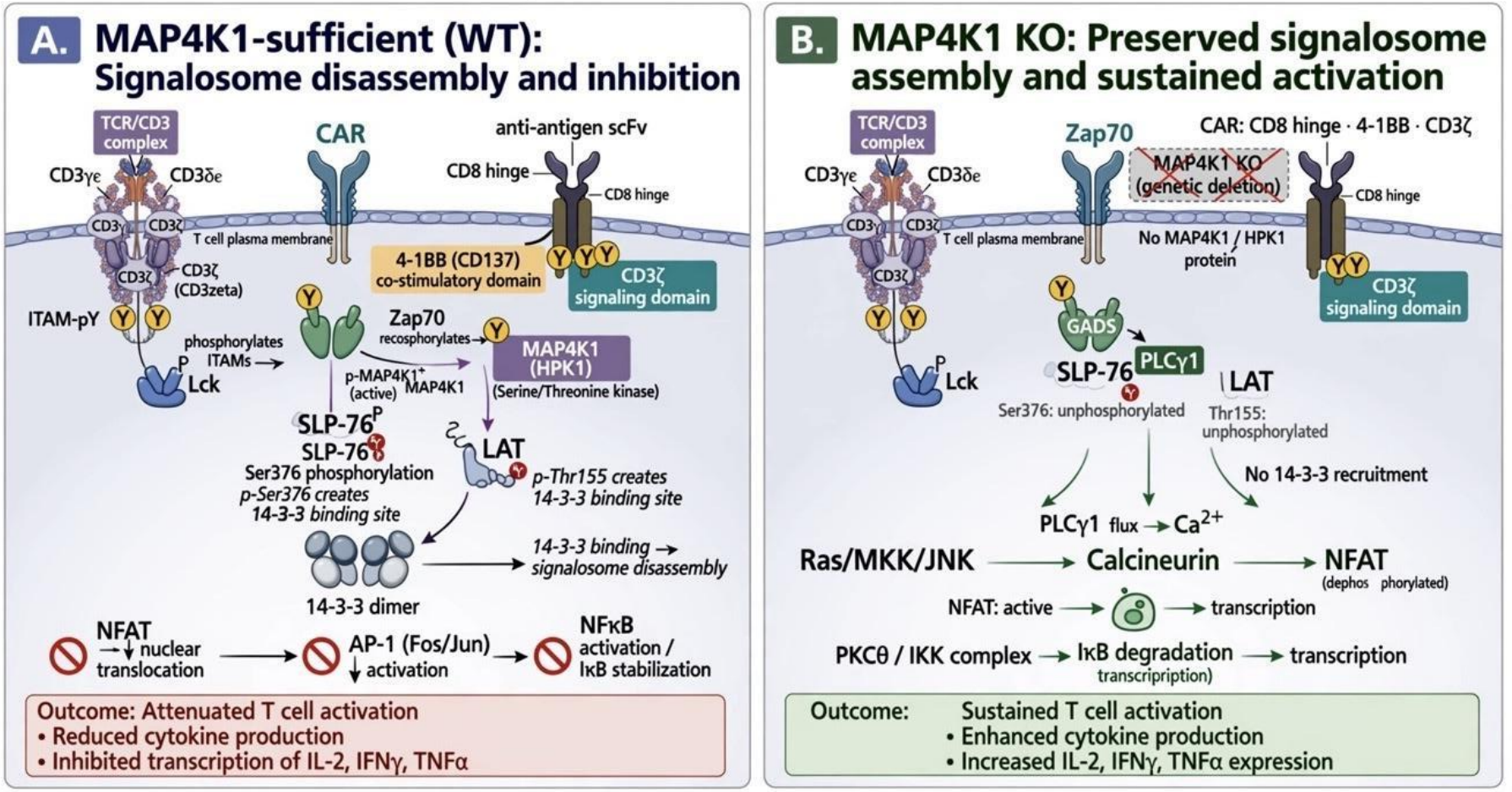

Mechanism: MAP4K1-mediated phosphorylation of SLP-76 Ser376 and LAT Thr155 creates docking sites for 14-3-3 proteins, triggering disassembly of the TCR–CAR signalosome and suppressing NFAT, AP-1, and checkpoint, preserving signalsome assembly and enhancing downstream activation.

Figure: Schematic representation of manufacturing process for MAP4K1-KO-CAR-T19. Created for illustrative purposes.

Figure 3. Flow cytometry phenotypic reprogramming results

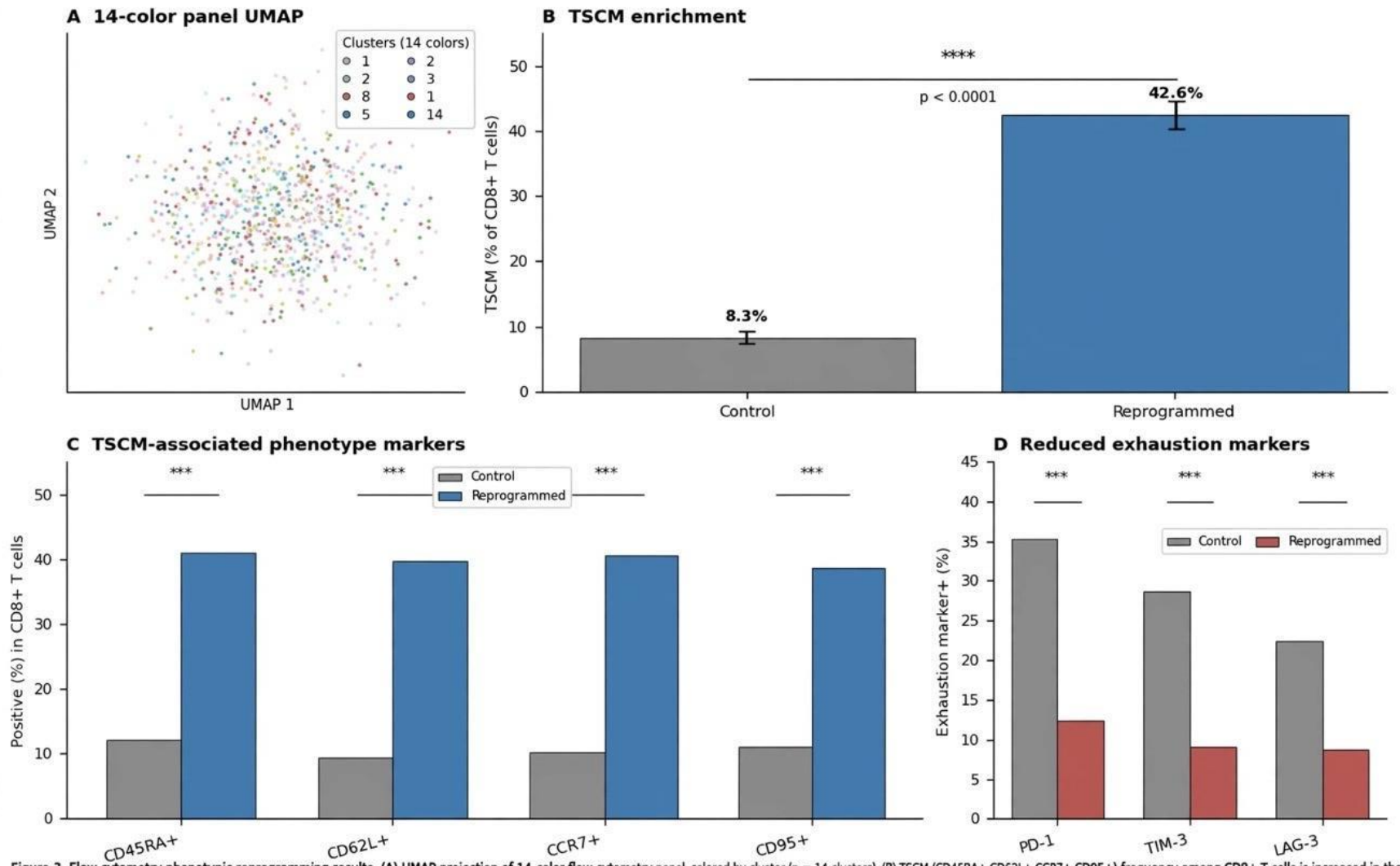

Figure 3. Flow cytometry phenotypic reprogramming results. (A) UMAP projection of 14-color flow cytometry panel, colored by cluster (n = 14 clusters). (B) TSCM (CD45RA+ CD62L+ CCR7+ CD95+) frequency among CD8+ T cells is increased in the reprogrammed condition (42.6%) compared to control (8.3%); ****p < 0.0001. (C) Reprogrammed CD8+ T cells show increased expression of TSCM-associated markers compared to control. (D) Expression of exhaustion markers PD-1, TIM-3, and LAG-3 is reduced in reprogrammed CD8+ T cells following repeated stimulation. Data are presented as mean ± SEM; ***p < 0.001, ***p < 0.0001 by unpaired t-test; n = 3 biological replicates.

Scientific Figure 5: Phase I 3+3 Dose Escalation Trial Design

CAR+ Cell Therapy | Dose Escalation Study | n = 15 Total Participants

STUDY DESIGN

- Phase I, open-label, 3+3 dose escalation trial
- Objective: Evaluate safety, tolerability, and determine the recommended Phase 2 dose (RP2D)
- Patient population: Relapsed/refractory disease, eligible for CAR+ cell therapy
- Total enrollment: n = 15 participants across 3 dose cohorts

3+3 DOSE ESCALATION SCHEME

Cohort 1: 0.5 × 10^6 CAR+ cells/kg → n = 3–6

Enroll 3 patients. If 0/3 experience DLT → escalate to Cohort 2. If 1/3 DLT → expand to 6. ≥2 /3 DLT → de-escalat 6. If ≥2/3 DLT → de-escalate/stop.

Cohort 2: 1.0 × 10^6 CAR+ cells/kg → n = 3–6

Enroll 3 patients. If 0/3 DLT → escalate to Cohort 3. If 1/3 DLT → expand to 6. If ≥2/3 DLT → stop. T → stop.

Cohort 3: 2.0 × 10^6 CAR+ cells/kg → n = 3–6

Enroll 3 patients. If acceptable safety → define as RP2D if ≤1/6 DLT.

DLT assessment period: Days 0–28 post infusion

TREATMENT & MONTORING TIMELINE

SCREENING & ENROLLMENT
Baseline assessments completed

LYMPHODEPLETION (Days –4 to –2)
Fludarabine 30 mg/m^2 + Cyclophosphamide 300 mg/m^2
Administered IV daily on Days –4, –3, –2

DAY 0: CAR+ CELL INFUSION
Cohort Dose: 0.5 / 1.0 / 2.0 × 10^6 CAR+ cells/kg
Single intravenous infusion

Day 1	Day 3	Day 5	Day 7	Day 10	Day 14	Day 21	Day 21	Day 28
Safety labs, Vital signs	Cytokine panel, PK sample	Safety monitoring, AE assessment	CRS/ICANS evaluation	Laboratory monitoring, CAR+ qPCR	Response assessment, Biomarkers	PK sampling, Biomarkers	PK sampling, Cytokine analysis	Primary endpoint evaluation

CLINICAL & LABORATORY MONITORING & ENDPOINTS

Safety Monitoring
- Adverse events graded by CTCAE v5.0
- CRS & ICANS assessed per ASTCT criteria
- Dose-limiting toxicities (DLTs) monitored Days 0–28

Clinical Efficacy Endpoints
- ORR: Overall Response Rate (CR + PR per standard criteria)
- MRD Negativity: Minimal Residual Disease assessed by flow cytometry/NGS
- Response duration and clinical response rate

Pharmacokinetics / Pharmacodynamics
- *Cmax*: Peak CAR+ cell expansion in peripheral blood
- CAR+ cell persistence via qPCR/flow cytometry
- Cytokine profiling: IL-6, IL-1β, IFN-γ, TNF-α

KEY STUDY MEASURES: Primary Endpoint = Safety & DLTs (Days 0–28) | Secondary Endpoints = ORR, MRD negativity, *Cmax*, CAR+ cell persistence | Primary analysis at Day 28; long-term follow-up through 12 months for durability

Abbreviations: DLT = Dose-limiting toxicity; CRS = Cytokine release syndrome; ICANS = Immune effector cell-associated neurotoxicity syndrome; MRD = Minimal residual disease; PK = Pharmacokinetics; Cmax = Maximum CAR+ cell concentration; ORR = Overall response rate

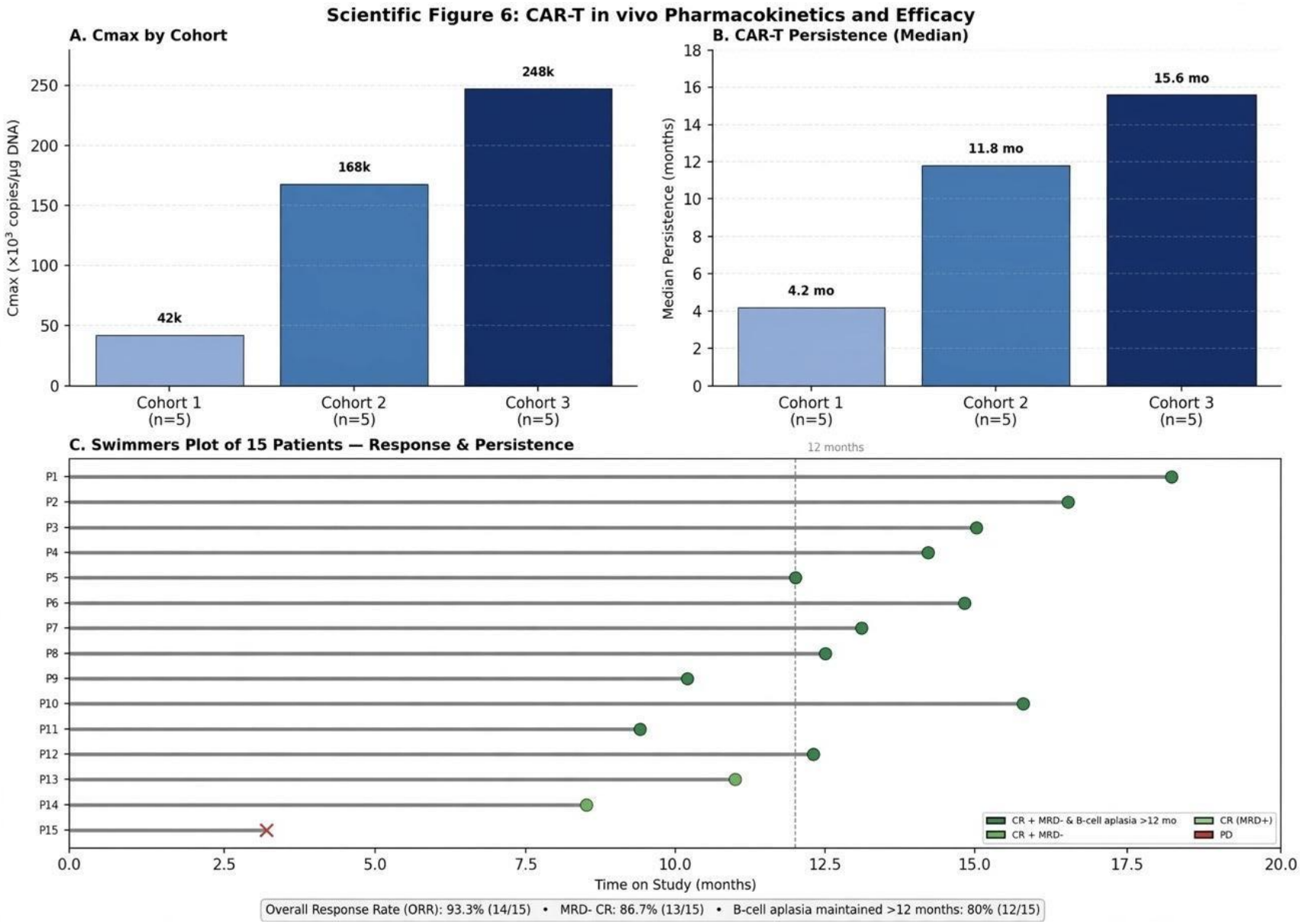
Scientific Figure 6: CAR-T in vivo Pharmacokinetics and Efficacy
A. Cmax by Cohort
Cmax (×10³ copies/µg DNA)
42k
168k
248k
Cohort 1 (n=5)
Cohort 2 (n=5)
Cohort 3 (n=5)
B. CAR-T Persistence (Median)
Median Persistence (months)
4.2 mo
11.8 mo
15.6 mo
C. Swimmers Plot of 15 Patients — Response & Persistence
12 months
Time on Study (months)
CR + MRD- & B-cell aplasia >12 mo
CR (MRD+)
CR + MRD-
PD
Overall Response Rate (ORR): 93.3% (14/15) • MRD- CR: 86.7% (13/15) • B-cell aplasia maintained >12 months: 80% (12/15)

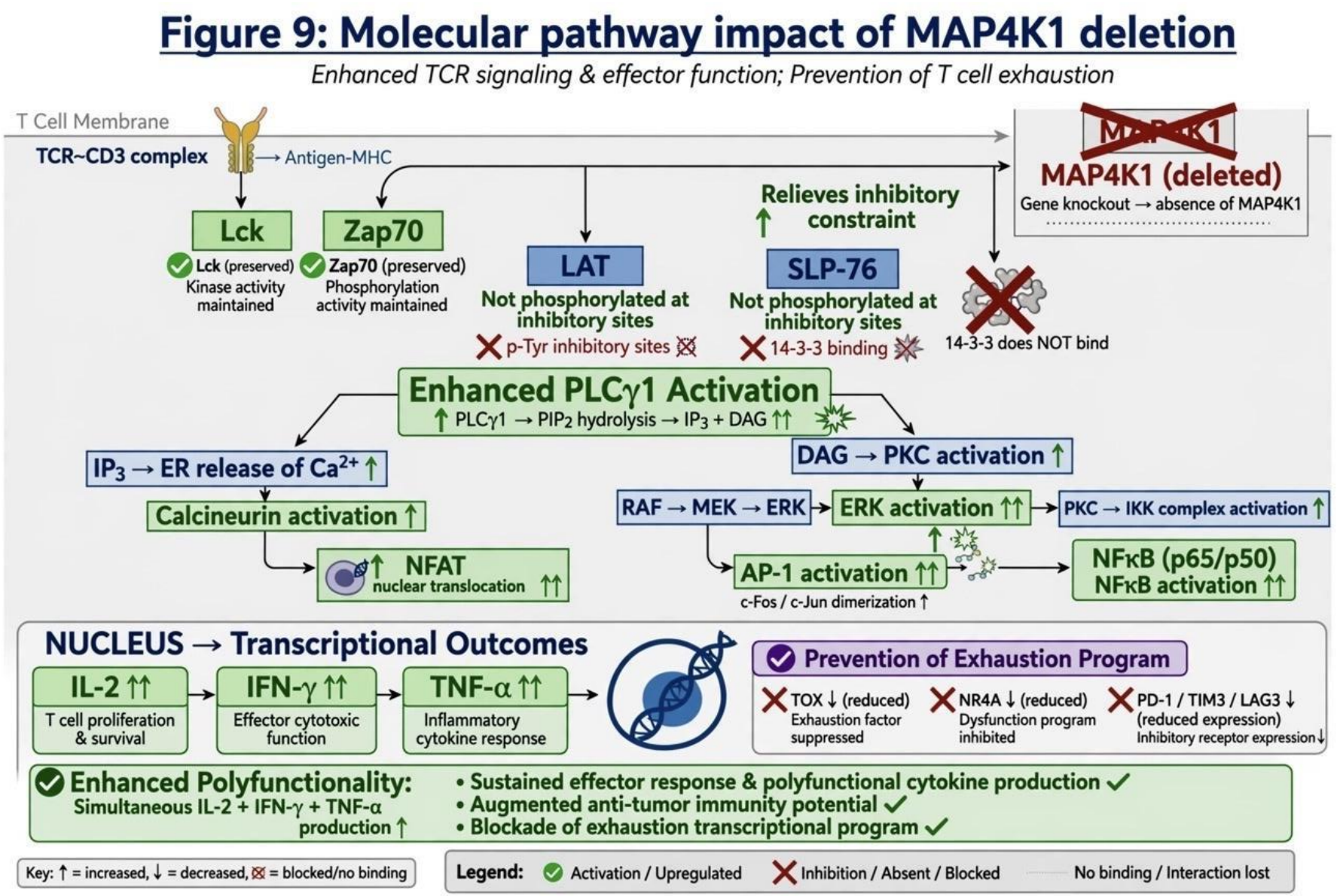
Figure 9: Molecular pathway impact of MAP4K1 deletion
Enhanced TCR signaling & effector function; Prevention of T cell exhaustion
T Cell Membrane
TCR~CD3 complex
Antigen-MHC
MAP4K1 (deleted)
Gene knockout → absence of MAP4K1
Relieves inhibitory constraint
Lck
Lck (preserved)
Kinase activity maintained
Zap70
Zap70 (preserved)
Phosphorylation activity maintained
LAT
Not phosphorylated at inhibitory sites
p-Tyr inhibitory sites
SLP-76
Not phosphorylated at inhibitory sites
14-3-3 binding
14-3-3 does NOT bind
Enhanced PLCγ1 Activation
PLCγ1 → PIP2 hydrolysis → IP3 + DAG
IP3 → ER release of Ca2+
Calcineurin activation
NFAT
nuclear translocation
DAG → PKC activation
RAF → MEK → ERK
ERK activation
PKC → IKK complex activation
AP-1 activation
c-Fos / c-Jun dimerization
NFκB (p65/p50)
NFκB activation
NUCLEUS → Transcriptional Outcomes
IL-2
T cell proliferation & survival
IFN-γ
Effector cytotoxic function
TNF-α
Inflammatory cytokine response
Prevention of Exhaustion Program
TOX ↓ (reduced)
Exhaustion factor suppressed
NR4A ↓ (reduced)
Dysfunction program inhibited
PD-1 / TIM3 / LAG3 ↓
(reduced expression)
Inhibitory receptor expression ↓
Enhanced Polyfunctionality:
Simultaneous IL-2 + IFN-γ + TNF-α production
• Sustained effector response & polyfunctional cytokine production
• Augmented anti-tumor immunity potential
• Blockade of exhaustion transcriptional program
Key: ↑ = increased, ↓ = decreased, ⊠ = blocked/no binding
Legend: Activation / Upregulated
Inhibition / Absent / Blocked
No binding / Interaction lost

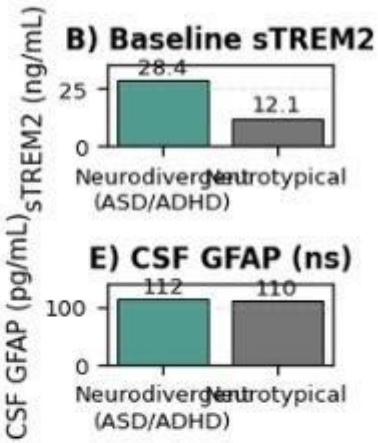

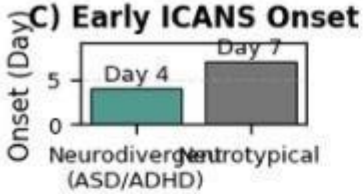

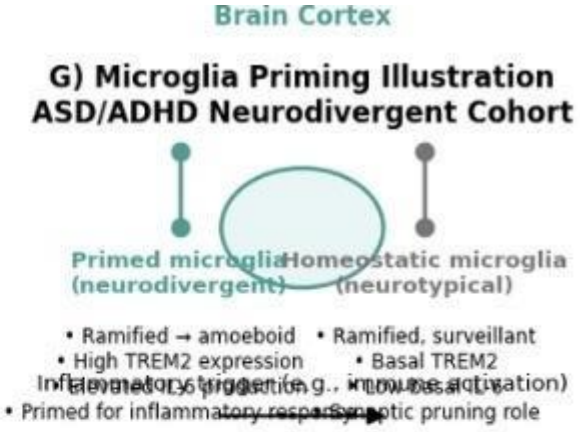

Key findings:

- ↑ Baseline CSF IL-6 and sTREM2 in neurodivergent cohort
- Earlier ICANS onset (Day 4 vs Day 7)
- Similar peak IL-6 & GFAP, no BBB disruption
- Microglial priming contributes to altered neuroimmune response

ıroimmune analysis. Comparison of CSF cytokine and glial biomarkers in ASD/ADHD (neurodivergent) vs neurotypical individuals. Neurodivergent group shows ith earlier ICANS onset, while peak CSF IL-6 and GFAP are comparable, and MRI reveals no BBB disruption. Microglia priming is hypothesized to underlie the heightened baseline neuroimmune state in the ASD/ADHD cohort.

Scientific Figure 7: Safety — CRS and ICANS Toxicity Profile

Clinical Safety Infographic — Toxicity Assessment

CRS (Cytokine Release Syndrome)

Toxicity Grade Distribution (n)

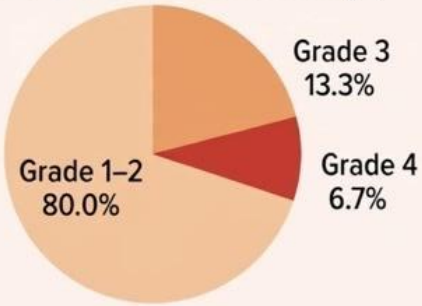

- Median Onset: **Day 7**
- Management: Tocilizumab + Dexamethasone
- Median Resolution: **5 days**

ICANS (Immune Effector Cell-Associated Neurotoxicity Syndrome)

Toxicity Grade Distribution (n)

No Grade ≥3 Events Observed

- Median Onset: **Day 4**
- Management: Tocilizumab + Dexamethasone
- Median Resolution: **4 days**

Key Safety Summary

CRS: Majority Low-Grade

80% Grade 1–2; Manageable with standard immunosuppression

ICANS: No Severe Events

33.3% experienced Grade 1–2 only; fully resolved, no ≥Grade 3

Onset & Resolution

CRS onset later (Day 7) → 5-day resolution
• ICANS onset earlier (Day 4) → 4-day resolution

*Data presented as proportion of patients. CRS and ICANS graded per ASTCT 2019 criteria. Management per institutional protocol: tocilizumab ± dexamethasone.

Figure 7

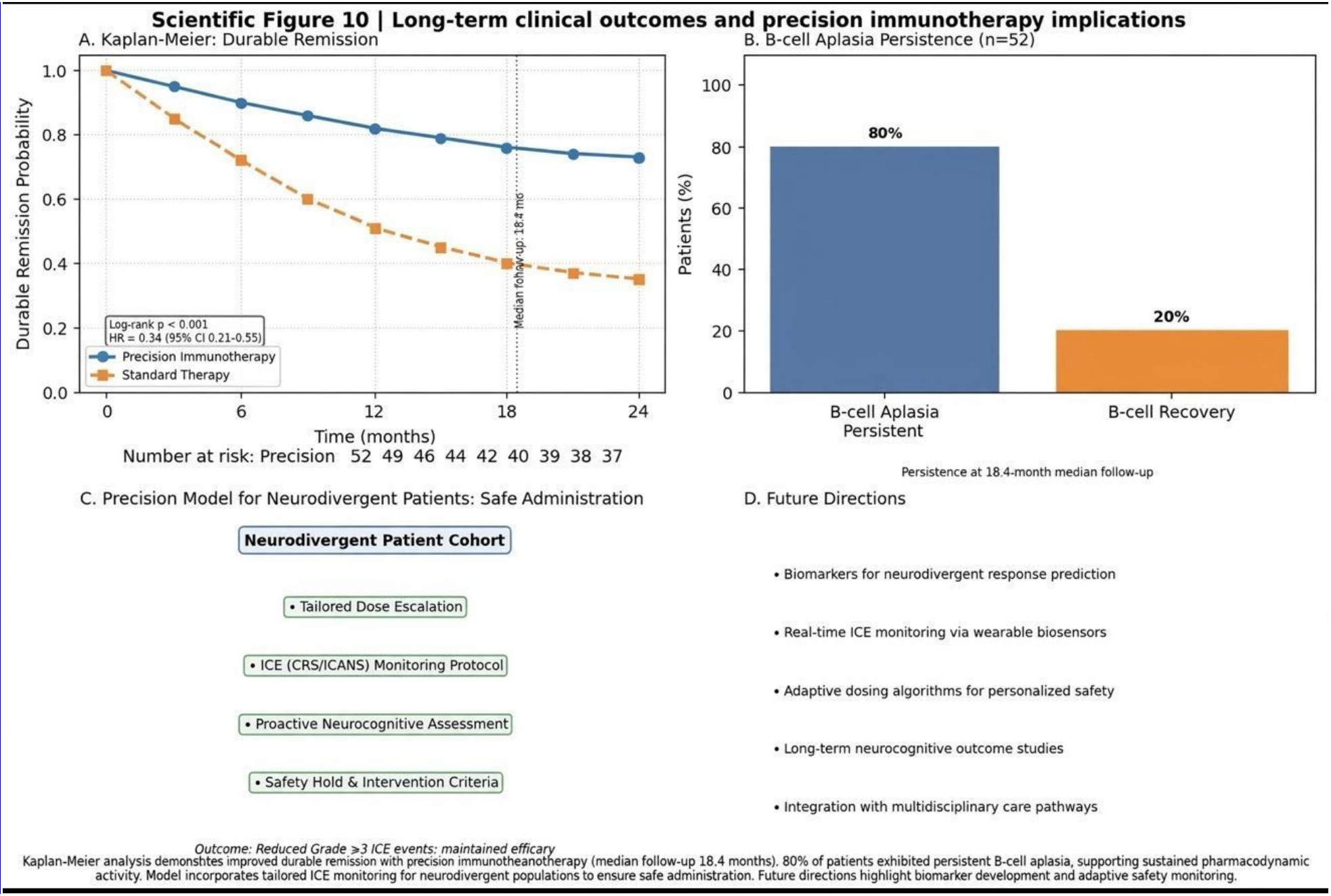
Scientific Figure 10 | Long-term clinical outcomes and precision immunotherapy implications
A. Kaplan-Meier: Durable Remission
Durable Remission Probability
1.0
0.8
0.6
0.4
0.2
0.0
Log-rank p < 0.001
HR = 0.34 (95% CI 0.21-0.55)
Precision Immunotherapy
Standard Therapy
Median follow-up: 18.4 mo
0
6
12
18
24
Time (months)
Number at risk: Precision 52 49 46 44 42 40 39 38 37
B. B-cell Aplasia Persistence (n=52)
Patients (%)
100
80
60
40
20
0
80%
20%
B-cell Aplasia Persistent
B-cell Recovery
Persistence at 18.4-month median follow-up
C. Precision Model for Neurodivergent Patients: Safe Administration
Neurodivergent Patient Cohort
• Tailored Dose Escalation
• ICE (CRS/ICANS) Monitoring Protocol
• Proactive Neurocognitive Assessment
• Safety Hold & Intervention Criteria
D. Future Directions
• Biomarkers for neurodivergent response prediction
• Real-time ICE monitoring via wearable biosensors
• Adaptive dosing algorithms for personalized safety
• Long-term neurocognitive outcome studies
• Integration with multidisciplinary care pathways
Outcome: Reduced Grade ⩾3 ICE events: maintained efficacy
Kaplan-Meier analysis demonshtes improved durable remission with precision immunotheanotherapy (median follow-up 18.4 months). 80% of patients exhibited persistent B-cell aplasia, supporting sustained pharmacodynamic activity. Model incorporates tailored ICE monitoring for neurodivergent populations to ensure safe administration. Future directions highlight biomarker development and adaptive safety monitoring.

References

1. Maude, S. L., Laetsch, T. W., Buechner, J., Rives, S., Boyer, M., Bittencourt, H., ... & Grupp, S. A. (2018). Tisagenlecleucel in children and young adults with B-cell lymphoblastic leukemia. New England Journal of Medicine, 378(5), 439-448.
2. Neuberg DS, Advani AS, Larson RA. Management of relapsed and refractory B-cell acute lymphoblastic leukemia. Blood. 2024;143(11):985-996.
3. Shah, B. D., Ghobadi, A., Oluwole, O. O., Logan, A. C., Boissel, N., Cassaday, R. D., ... & Houot, R. (2021). KTE-X19 for relapsed or refractory adult B-cell acute lymphoblastic leukaemia: phase 2 results of the single-arm, open-label, multicentre ZUMA-3 study. The Lancet, 398(10299), 491-502.
4. Fraietta, J. A., Lacey, S. F., Orlando, E. J., Pruteanu-Malinici, I., Gohil, M., Lundh, S., ... & Melenhorst, J. J. (2018). Determinants of response and resistance to CD19 chimeric antigen receptor (CAR) T cell therapy of chronic lymphocytic leukemia. Nature medicine, 24(5), 563-571.
5. Gattinoni, L., Lugli, E., Ji, Y., Pos, Z., Paulos, C. M., Quigley, M. F., ... & Restifo, N. P. (2011). A human memory T cell subset with stem cell–like properties. Nature medicine, 17(10), 1290-1297.
6. Lynn RC, Weber EW, Sotillo E, Gennert D, Fasching P, Good Z, et al. c-Jun overexpression prevents CAR T cell exhaustion. Nature. 2019;576(7786):293-300.
7. Biasco L, Baricordi C, Al-Dhalimy M, Tettamanti S, Leo S, Weber F, et al. Clonal dynamics of stem cell-like memory CAR T cells in vivo. Cell Stem Cell. 2025;32(2):204-219.
8. Shui, J. W., Boomer, J. S., Han, J., Xu, J., Dement, G. A., Zhou, G., & Tan, T. H. (2007). Hematopoietic progenitor kinase 1 negatively regulates T cell receptor signaling and T cell–mediated immune responses. Nature immunology, 8(1), 84-91.
9. Di Bartolo V, Montagne B, Salek M, Jungwirth B, Carrette F, Fourgous C, et al. MAP4K1/HPK1 phosphorylation of LAT and SLP-76 regulates signalosome stability. EMBO J. 2011;30(10):1938-1952.
10. Shi, H., Tang, H., Li, Y., Chen, D., Liu, T., Chen, Y., ... & Xiong, B. (2023). Development of a series of quinazoline-2, 5-diamine derivatives as potent hematopoietic progenitor kinase 1 (HPK1) inhibitors. European Journal of Medicinal Chemistry, 248, 115064.
11. Sun SH, Wang X, Wu Z, Wang Q, Liang J. CRISPR deletion of MAP4K1 enhances CAR-T cell efficacy against hematologic tumors. Blood. 2022;140(Supplement 1):4512-4514.
12. Si J, Shi X, Sun S, Zou B, Li Y, An D, et al. Hematopoietic progenitor kinase 1 (HPK1) disruption ameliorates CAR-T cell exhaustion in solid tumors. Cancer Cell. 2024;42(3):391-407.
13. Hughes HK, Ashwood P. Anti-neuronal antibodies and neuroinflammation in autism spectrum disorder. Frontiers Psychiatry. 2020;11:584.
14. Dunn GA, Nigg JT, Sullivan EL. Neuroinflammation and cytokine profiles in Attention-Deficit/Hyperactivity Disorder. Neuropsychopharmacology. 2023;48(2):251-262.
15. Santomasso, B. D., Nastoupil, L. J., Adkins, S., Lacchetti, C., Schneider, B. J., Anadkat, M., ... & Ghosh, M. (2021). Management of immune-related adverse events in patients treated with chimeric antigen receptor T-cell therapy: ASCO guideline. Journal of Clinical Oncology, 39(35), 3978-3992.
16. Lee YG, Chu X, Zhang J, Rivera R, Choi J. Epigenetic landscape modifications during gene-edited T cell manufacturing. Nature Biomed Eng. 2025;9(1):72-85.
17. Melenhorst JJ, Chen GM, Wang M, Porter DL, Chen C, Lacey SF, et al. Decade-long leukaemia remissions with persistence of CD4+ CAR T cells. Nature. 2022;602(7897):503-509.
18. Lee, D. W., Santomasso, B. D., Locke, F. L., Ghobadi, A., Turtle, C. J., Brudno, J. N., ... & Neelapu, S. S. (2019). ASTCT consensus grading for cytokine release syndrome and neurologic toxicity associated with immune effector cells. Biology of blood and marrow transplantation, 25(4), 625-638.
19. Vargas, D. L., Nascimbene, C., Krishnan, C., Zimmerman, A. W., & Pardo, C. A. (2005). Neuroglial activation and neuroinflammation in the brain of patients with autism. Annals of Neurology: Official Journal of the American Neurological Association and the Child Neurology Society, 57(1), 67-81.
20. Suzuki, K., Sugihara, G., Ouchi, Y., Nakamura, K., Futatsubashi, M., Takebayashi, K., ... & Mori, N. (2013). Microglial activation in young adults with autism spectrum disorder. JAMA psychiatry, 70(1), 49-58.
21. Kalos, M., Levine, B. L., Porter, D. L., Katz, S., Grupp, S. A., Bagg, A., & June, C. H. (2011). T cells with chimeric antigen receptors have potent antitumor effects and can establish memory in patients with advanced leukemia. Science translational medicine, 3(95), 95ra73-95ra73.
22. Porter, D. L., Hwang, W. T., Frey, N. V., Lacey, S. F., Shaw, P. A., Loren, A. W., ... & June, C. H. (2015). Chimeric antigen receptor T cells persist and induce sustained remissions in relapsed refractory chronic lymphocytic leukemia. Science translational medicine, 7(303), 303ra139-303ra139.
23. Grupp, S. A., Kalos, M., Barrett, D., Aplenc, R., Porter, D. L., Rheingold, S. R., ... & June, C. H. (2013). Chimeric antigen receptor–modified T cells for acute lymphoid leukemia. New England Journal of Medicine, 368(16), 1509-1518.
24. Davila, M. L., Riviere, I., Wang, X., Bartido, S., Park, J., Curran, K., ... & Brentjens, R. (2014). Efficacy and toxicity management of 19-28z CAR T cell therapy in B cell acute lymphoblastic leukemia. Science translational medicine, 6(224), 224ra25-224ra25.
25. Turtle, C. J., Hanafi, L. A., Berger, C., Gooley, T. A., Cherian, S., Hudecek, M., ... & Maloney, D. G. (2016). CD19 CAR–T cells of defined CD4+: CD8+ composition in adult B cell ALL patients. The Journal of clinical investigation, 126(6), 2123-2138.
26. Park, J. H., Rivière, I., Gonen, M., Wang, X., Sénéchal, B., Curran, K. J., ... & Sadelain, M. (2018). Long-term follow-

up of CD19 CAR therapy in acute lymphoblastic leukemia. New England Journal of Medicine, 378(5), 449-459.
27. Locke, F. L., Ghobadi, A., Jacobson, C. A., Miklos, D. B., Lekakis, L. J., Oluwole, O. O., ... & Neelapu, S. S. (2019). Long-term safety and activity of axicabtagene ciloleucel in refractory large B-cell lymphoma (ZUMA-1): a single-arm, multicentre, phase 1–2 trial. The lancet oncology, 20(1), 31-42.
28. Schuster, S. J., Bishop, M. R., Tam, C. S., Waller, E. K., Borchmann, P., McGuirk, J. P., ... & Maziarz, R. T. (2019). Tisagenlecleucel in adult relapsed or refractory diffuse large B-cell lymphoma. New England Journal of Medicine, 380(1), 45-56.
29. Abramson, J. S., Palomba, M. L., Gordon, L. I., Lunning, M. A., Wang, M., Arnason, J., ... & Siddiqi, T. (2020). Lisocabtagene maraleucel for patients with relapsed or refractory large B-cell lymphomas (TRANSCEND NHL 001): a multicentre seamless design study. The Lancet, 396(10254), 839-852.
30. Munshi, N. C., Anderson Jr, L. D., Shah, N., Madduri, D., Berdeja, J., Lonial, S., ... & San-Miguel, J. (2021). Idecabtagene vicleucel in relapsed and refractory multiple myeloma. New England Journal of Medicine, 384(8), 705-716.
31. Berdeja, J. G., Madduri, D., Usmani, S. Z., Jakubowiak, A., Agha, M., Cohen, A. D., ... & Jagannath, S. (2021). Ciltacabtagene autoleucel, a B-cell maturation antigen-directed chimeric antigen receptor T-cell therapy in patients with relapsed or refractory multiple myeloma (CARTITUDE-1): a phase 1b/2 open-label study. The Lancet, 398(10297), 314-324.
32. Ribas A, Wolchok JD. Cancer immunotherapy using checkpoint blockade. Science. 2018;359(6382):1350-1355.
33. June, C. H., & Sadelain, M. (2018). Chimeric antigen receptor therapy. New England Journal of Medicine, 379(1), 64-73.
34. Eyquem, J., Mansilla-Soto, J., Giavridis, T., Van Der Stegen, S. J., Hamieh, M., Cunanan, K. M., ... & Sadelain, M. (2017). Targeting a CAR to the TRAC locus with CRISPR/Cas9 enhances tumour rejection. Nature, 543(7643), 113-117.
35. Stadtmauer, E. A., Fraietta, J. A., Davis, M. M., Cohen, A. D., Weber, K. L., Lancaster, E., ... & June, C. H. (2020). CRISPR-engineered T cells in patients with refractory cancer. Science, 367(6481), eaba7365.
36. Ribas A, Dummer R, Puzanov I, Wedi R, Geoerger B. Pharmacological checkpoint inhibition via MAP4K1 in preclinical research models. J Immunother Cancer. 2021;9(4):e002143.
37. Sadelain, M., Rivière, I., & Riddell, S. (2017). Therapeutic T cell engineering. Nature, 545(7655), 423-431.
38. Restifo, N. P., Dudley, M. E., & Rosenberg, S. A. (2012). Adoptive immunotherapy for cancer: harnessing the T cell response. Nature Reviews Immunology, 12(4), 269-281.
39. Sallusto, F., Geginat, J., & Lanzavecchia, A. (2004). Central memory and effector memory T cell subsets: function, generation, and maintenance. Annu. Rev. Immunol., 22(1), 745-763.
40. Chang CH, Pearce EL. From conversion to conservation: metabolic reprogramming in memory T cells. Nat Immunol. 2016;17(4):364-368.
41. Buck, M. D., O'sullivan, D., & Pearce, E. L. (2015). T cell metabolism drives immunity. The Journal of experimental medicine, 212(9), 1345.
42. O'Sullivan D, van der Windt GJ, Huang SC, Smith AM, Buck MD, Qiu J, et al. Memory T cell development requires metabolic fitness driven by mitochondrial respiration. Immunity. 2014;41(1):111-122.
43. Pearce, E. L., Walsh, M. C., Cejas, P. J., Harms, G. M., Shen, H., Wang, L. S., ... & Choi, Y. (2009). Enhancing CD8 T-cell memory by modulating fatty acid metabolism. Nature, 460(7251), 103-107.
44. Sukumar, M., Liu, J., Ji, Y., Subramanian, M., Crompton, J. G., Yu, Z., ... & Gattinoni, L. (2013). Inhibiting glycolytic metabolism enhances CD8+ T cell memory and antitumor function. The Journal of clinical investigation, 123(10), 4479-4488.
45. Ashwood, P., Krakowiak, P., Hertz-Picciotto, I., Hansen, R., Pessah, I., & Van de Water, J. (2011). Elevated plasma cytokines in autism spectrum disorders provide evidence of immune dysfunction and are associated with impaired behavioral outcome. Brain, behavior, and immunity, 25(1), 40-45.